
**Comments on Inorganic Chemistry**
Publication details, including instructions for authors and subscription information:
http://www.informaworld.com/smpp/title~content=t713455155

# Electrochemistry and Catalysis by Myoglobin in Surfactant Films

Patrick J. Farmer[a]; Rong Lin[a]; Mekki Bayachou[a]
[a] Department of Chemistry, University of California Irvine, Irvine, California, USA

**To cite this Article** Farmer, Patrick J. , Lin, Rong and Bayachou, Mekki(1998) 'Electrochemistry and Catalysis by Myoglobin in Surfactant Films', Comments on Inorganic Chemistry, 20: 2, 101 — 120
**To link to this Article: DOI:** 10.1080/02603599808012254
**URL:** http://dx.doi.org/10.1080/02603599808012254

# Electrochemistry and Catalysis by Myoglobin in Surfactant Films

PATRICK J. FARMER
RONG LIN and MEKKI BAYACHOU

*Department of Chemistry,*
*University of California, Irvine,*
*Irvine, California 92697–2025 USA*

(Received 11 August, 1997)

The electrochemical response of myoglobin and its metal-substituted or chemically modified derivatives is greatly enhanced when contained within surfactant films on electrode surfaces. The aqueous electrochemistry of such myoglobin-films is similar to that of Fe-porphyrins in organic solvents in that both $Fe^{III/II}$ and $Fe^{II/I}$ couples are chemically reversible, but aqueous phase ligands readily interact with the Fe site. Sequential and rapid scanning voltammetry yield dynamic electrochemistry indicative of gating of electron transfer by ligand dissociation and active site rearrangement. These myoglobin/surfactant films have biomimetic nitrite-, sulfite- and oxido-reductase activity. Initial investigations into nitrite reductions catalyzed by the myoglobin-films are described. A nitroxyl intermediate. $Fe^{II}$-$NO^-$, is the likely branching point between different pathways forming $NH_3$ and $N_2O$.

Keywords: *electrochemistry, myoglobin, surfactant, reductive catalysis, nitrite, nitroxyl*



## INTRODUCTION

Heme proteins catalyze a number of vital multi-electron reductions: the four electron reduction of $O_2$ to $H_2O$, the two-electron reduction of $O_2$

*Comments Inorg. Chem.*
1998, Vol. 20, No. 2-3, pp. 101-120
Reprints available directly from the publisher
Photocopying permitted by license only

resulting in incorporation of an O-atom stereospecifically into a substrate, and the six-electron reductions of $NO_2^-$ and $SO_3^{2-}$ to $NH_4^+$ and $H_2S$, respectively.[1-4] A general feature of these complex, proton-coupled, multi-electron processes is that the required electrons are delivered to the enzyme from single-electron donors.[5] A second common feature is the 2-electron cleavage of water from an FeXO species (where X is O, N, or S) (Scheme 1).

| | |
|---|---|
| $O_2 + 4\,e^- + 4\,H^+ \longrightarrow 2\,H_2O$ | cytochrome c oxidase |
| $RH + O_2 + 2\,e^- + 2\,H^+ \longrightarrow ROH + H_2O$ | cytochrome p450 |
| $NO_2^- + 6\,e^- + 8\,H^+ \longrightarrow NH_4^+ + 2\,H_2O$ | nitrite reductase |
| $SO_3^{2-} + 6\,e^- + 8\,H^+ \longrightarrow H_2S + 3\,H_2O$ | sulfite reductase |

SCHEME 1



It would seem logical to examine such reactions by electrochemistry, where the potential and kinetics of sequential reductions can be followed and product formation matched to catalyst oxidation state.[6] In general though, the sluggish electrochemical response of redox proteins to standard techniques makes mult-electron catalysis difficult to initiate and follow. Within the last ten years, however, dramatic advances in the direct electrochemistry of redox proteins have been made.[7-10] The major barrier has been in poor electron transfer between the electrode surface and the protein. Successful techniques used to overcome this problem include adsorption[9] or covalent attachment[10] of the protein to the electrode surface, and the use of promoters[8c] which coat the electrode surface with chemical functionalities that can directly interact with the protein.

To this end, Rusling has developed the use of water-insoluble surfactant films deposited on the electrode surface.[11-14] These films form stable, multilayer macrostructures which promote the rapid electrochemical response of redox active species contained within them.[11] Such systems are best described as biphasic, having both aqueous and hydrophobic regions, much like that of the phospholipid membranes in

which many important biological redox transformations occur. Rusling has used reversible electrochemical reductions of myoglobin (Mb),[11,12] cobalamin[13] and recently cytochrome P450[14] in these film electrodes to electrocatalytically dehalogenate chlorinated and brominated hydrocarbons.

By employing Mb within such films as an electroactive hemeprotein model, we hope to follow the mechanistic sequences of redox transformations in Scheme 1 electrochemically. Of particular interest is the nature and reactivity of partially reduced intermediates in the reductive processes. This Comment will describe two aspects of our work using this system. First, we describe the use of chemically modified and metal-substituted Mb film electrodes to gain insight into the protein electrochemistry within this unique environment. Then preliminary investigations are presented of the biomimetic reduction of nitrite catalyzed by the electroactive Mb in such films.

## MYOGLOBIN ELECTROCHEMISTRY IN DDAB FILMS



Layered films of surfactants such as dimethyldidodecylammonium bromide (ddab) on pyrolytic graphite (PG) adsorb Mb from solution to form stable Mb/ddab films.[11,12] The direct electrochemical response of Mb in these Mb/ddab films deposited on graphite, gold or platinum electrodes is greatly enhanced compared to that of Mb in aqueous solution.[15] Two electrochemical reductions from ferric Mb are seen in the cyclic voltammogram (CV) in Fig. 1, the first assigned to the $Fe^{III/II}$ couple, and a second couple tentatively assigned to $Fe^{II/I}$.[11c]

We have examined the electrochemical behavior of these Mb/ddab films, as well as those made with metal-substituted and chemically modified Mb. The $Fe^{III/II}$ potential of Mb in the film is somewhat lower than that determined by indirect, solution-based measurements (-250 mV vs. SCE, pH 7), but well within the range of values reported for direct determinations of Mb using chemically modified electrodes.[15] Coulometry consistently shows that 25 to 50% of the Mb in the film is electrochemically active. In our hands, a prepared electrode is stable to repeated cycling, can be moved from solution to solution, and with proper storage will remain active for over two weeks.

Electron transfer in Mb/ddab films follows diffusion-like kinetics in that, above 500 mV/s scan-rate, the current is proportional to the (scan

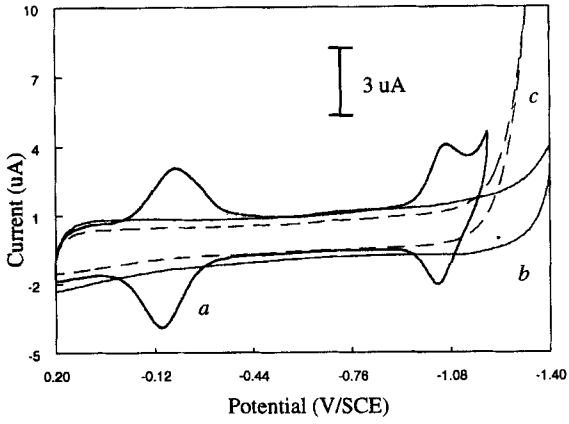


FIGURE 1 Cyclic voltammogram at 100 mV/s in pH 5.5 acetate buffer. 0.05 M NaBr of (a) Mb/ddab film on PG; (b) ddab film on PG; (c) PG



rate)$^{1/2}$. Such behavior could be due to Mb diffusion towards the electrode surface in a fluid film or to electron hopping between Mb sites in a more constrained environment.[16] The temperature dependence for Mb current-response follows that for the solid-to-liquid-crystal phase transition for ddab films; thus Rusling has proposed that the Mb diffuse between disordered liquid-crystalline bilayers, as depicted in Fig. 2.[12c] Several preparation procedures, including casting or spraying Mb/surfactant mixtures onto substrates and adsorbing Mb from solution into precast surfactant films, lead to essentially the same electrochemical behavior.[12] This adds credence to the fluid quality of these films once immersed in aqueous solutions.

The spectrochemical characterization of the second reduction as forming $Fe^{I}$ is based on the observed single Soret peak[11c] at 411 nm, but this is unlike that of the split Soret previously characterized for $Fe^{I}$ porphyrins (e.g., at 420 and 390 nm for $Fe^{I}$(TPP)).[17] No EPR data is yet available to confirm the Fe-based reduction, but metal substitutions allow an indirect assignment.[17c] If the added electron fills an empty porphyrin-based $\pi^*$ orbital, the potential should be somewhat insensitive to the nature of the metal; similar reduction waves may then be expected for films made with the Mn-, Co- and Zn-substituted Mb derivatives. In

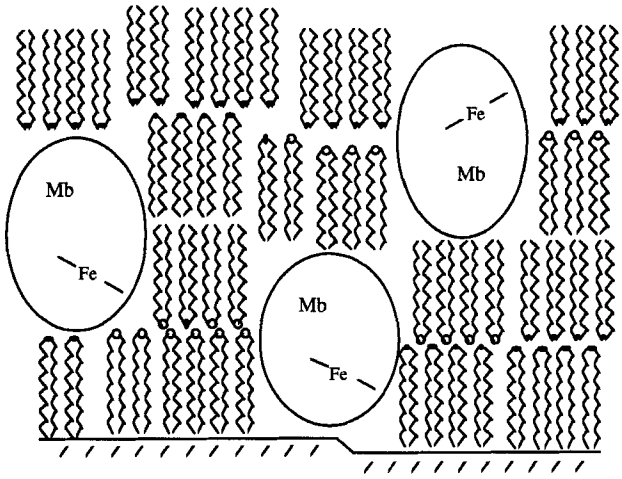


FIGURE 2 Model of Mb/ddab film from Ref. 12c



fact, reduction waves seen for the Mn- and Co-substituted Mbs are at very different potentials from that of the second Mb reduction, as expected for electron addition into different d-metal subshells (Table I). No reduction peak is seen for films made with ZnMb before the solvent reduction, as would be expected from the difference between Zn(TPP) and Fe(TPP) reduction of over 150 mV.[18] Likewise, no redox couple is seen for apoMb deposited in the films.

TABLE I Potentials for metal substituted Mb/ ddab films at pH 7.[a]

| | $M^{III/II}$(mV/SCE) | $M^{II/I}$(mV/SCE) |
|---|---|---|
| Mb | -222 | -1020 |
| CoMb | | -905 |
| MnMb | -273 | -- |
| ZnMb | - | -- |

a) Metal substituted Mb synthesized as in Refs. 19 and 20.

The electrochemical response seen for Mb/ddab films resembles that of Fe porphyrins in organic rather than aqueous solution. While the Mb/ddab films have reversible $Fe^{II/I}$ reductions, water soluble Fe-porphyrins show only irreversible reductions to the $Fe^{I}$ state, taken as evidence for the reaction of this state with water.[21a,b] Still, aqueous ions such as $CN^-$ and $N_3^-$ as well as $NO_2^-$ and $SO_3^{2-}$ interact readily with the Fe center in Mb/ddab, as evidenced by the shift in the $Fe^{III/II}$ reduction potential in their presence (Fig. 3). Likewise, the Soret band energies of the ferric-Mb/ddab films on glass or quartz shift to values similar to that of the solution-based adducts when immersed in ligand solutions (Table II).

TABLE II Comparison of Soret absorbances and $E_{1/2}$ values

| | *Ferric Soret (nm)* | | *$Fe^{III/II}$ (mV/SCE)* | |
|---|---|---|---|---|
| | *Solution* | *Film*[a] | *Solution* | *Film*[a] |
| Mb | 409 | 410 | -186[b] | -222 |
| Mb-$CN^-$ | 423[c] | 425 | -649[d,e] | -359[e] |
| Mb-$N_3^-$ | 421[c] | 419 | | -282 |
| Mb-$NO_2$ | 412[c] | 412 | | -235 |
| TzMb | 420[f] | 418 | -434[f] | -320[g] |
| Hemin | 390 | 388 | -307[h] | -242 |

[a] This work; [b] Ref. 22; [c] Ref. 23; [d] Ref 24; [e] pH 9.0; [f] Ref. 25a; [g] Determined by OSWV; [h] Ref. 16a.



Published EPR and electronic absorbance spectra indicate that the ferric Mb-heme site in ddab film retains proximal His-F8 ligation as in its native state.[12] But what of the distal pocket, where ligand-binding and catalysis should take place? As a specific probe of heme pocket structure, we utilized a modified myoglobin, TzMb, in which a chemically appended tetrazolyl-ligand binds to $Fe^{III}$ from the distal pocket (Fig. 4).[25] Its distinctive red color is retained in films on quartz, and is much different from that of Mb or hemin (Fe protoporphyrin IX cofactor), as illustrated in Fig. 4. Likewise, its steady-state reduction potential is shifted from that of Mb (Table II). These data suggest that the distal

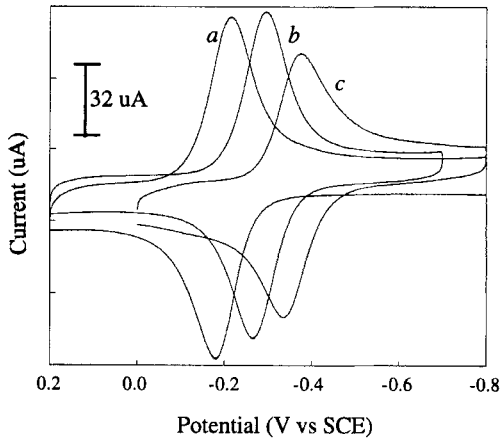


FIGURE 3 The same Mb/ddab electrode in (a) pH 7.0 phosphate buffer; (b) ca. 50 mM $NaN_3$; (c) pH 9.0, 50 mM NaCN



pocket residues remain in close proximity to the Fe center, more proof that a native-like structure is retained in the films. However, by comparison with the solution-based equilibrium potentials given in Table II, the overall heme environment is clearly different in the films.

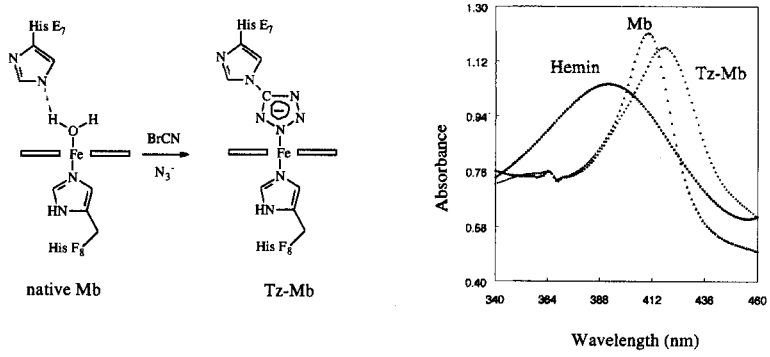


FIGURE 4 TzMb formation and UV-vis comparison between myoglobin, TzMb and hemin

The $Fe^{III/II}$ couple of the TzMb as determined by OSWV becomes ca. 20 mV more positive after repeated scans; the initial scan can be reproduced only after a long (>10 sec) oxidation at $Fe^{III}$ potentials. Such transient behavior, also seen for native Mb, is best illustrated by the change between sequential CV scans (Fig. 5). We interpret this behavior as a reduction-induced ligand dissociation, in effect a potential gating of the initial electron transfer.[26] Support for this view is the lack of such change in the presence of cyanide, which is known to bind to both ferric and ferrous Mb.[22]

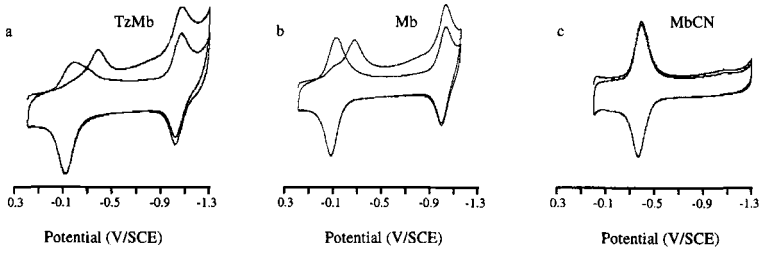


FIGURE 5 Sequential voltammograms of (a) TzMb, pH 7.0; (b) Mb, pH 7.0; (c) MbCN, pH 9.0. Conditions: at 500 mV/sec, 0.05 M NaBr



Full potential gating in TzMb is lost after the first scan at rates of greater than 0.1 V/s; the second and following scans show reproducible oxidation and reduction waves up to 200 mV/s, indicating fast electron transfer to the non-gated, 5-coordinate state. At very slow scan speeds (ca. 0.005 V/s) we obtain unchanged sequential CVs; these data are more comparable with that from indirect, steady-state potential determinations. Equilibration of TzMb after a reduction/oxidation cycle results in pH dependent mixtures of bound and unbound tetrazolyl states, similar to the behavior of TzMb in solution.[25c]

For Mb in solution, reduction to the ferrous state is accompanied by the loss of an axial-bound water,[25] and rebinding upon oxidation has been noted to be slow.[24] From the time required to reproduce the initial scan after reduction/oxidation, we estimate the rebinding to be on the order of seconds. Ligand-binding preferences in Fe-porphyrins change significantly with oxidation state; the tendency for σ-donor ligand loss upon reduction that is seen in Fe-porphyrin complexes is found in Mb/ddab as well.[18] From the effects of ligand concentrations on the

reduction potentials, sequential reduction from $Fe^{III}$ to $Fe^{II}$ to $Fe^{I}$ tends to result in sequential loss of axial ligation. Note that strong $CN^-$ binding to the ferrous state inhibits the second reduction wave (Fig. 5), further proof that this is a metal rather than a porphyrin-based reduction.

Qualitatively different electrochemical behavior is obtained with MnMb/ddab. Only small changes between sequential scans are seen, but there is a large difference in reduction and oxidation kinetics (Fig. 6). A qualitative scan rate study indicates a slow rearrangement following reduction; by increasing the scan rate, we can trap the unstable reduced form and reoxidize it before the rearrangement. A square scheme results (Scheme 2) in which a reduction-induced reorganization has a larger activation energy than the reorganization following oxidation.[7] From the scan rates needed to isolate the initial reversible oxidation of the unstable $Mn^{II}$Mb intermediate state, an estimated lifetime of ca. 40 ms is obtained.

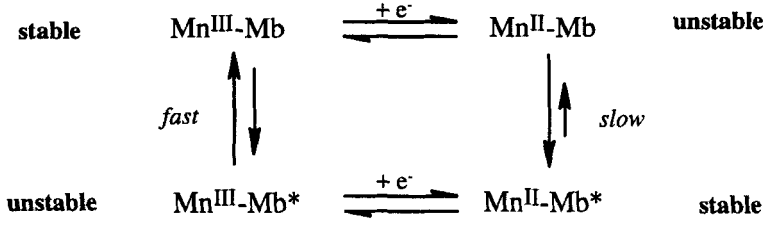


SCHEME 2

This dynamic behavior of Mn-Mb must be due to cofactor/protein interactions, as Mn-protoporphyrin IX (MnPP) in ddab/PG film has a quasi-reversible electrochemical behavior (i.e., comparable, though slow reduction and oxidation kinetics) very similar to that of Mn(TPP) in nonaqueous solvent (Fig 6).[27] The Mn(TPP) quasi-reversibility has been attributed to an increase in ion radius upon reduction, causing its displacement and a porphyrin core expansion. Interestingly, resonance Raman spectroscopy of reduced Mn-Mb revealed an unusual weakening of the proximal His-Mn bond, thought to be caused by steric crowding or heme pocket misfit.[28] We are pursuing efforts to identify the nature of the rearrangement in the MnMb/ddab films.

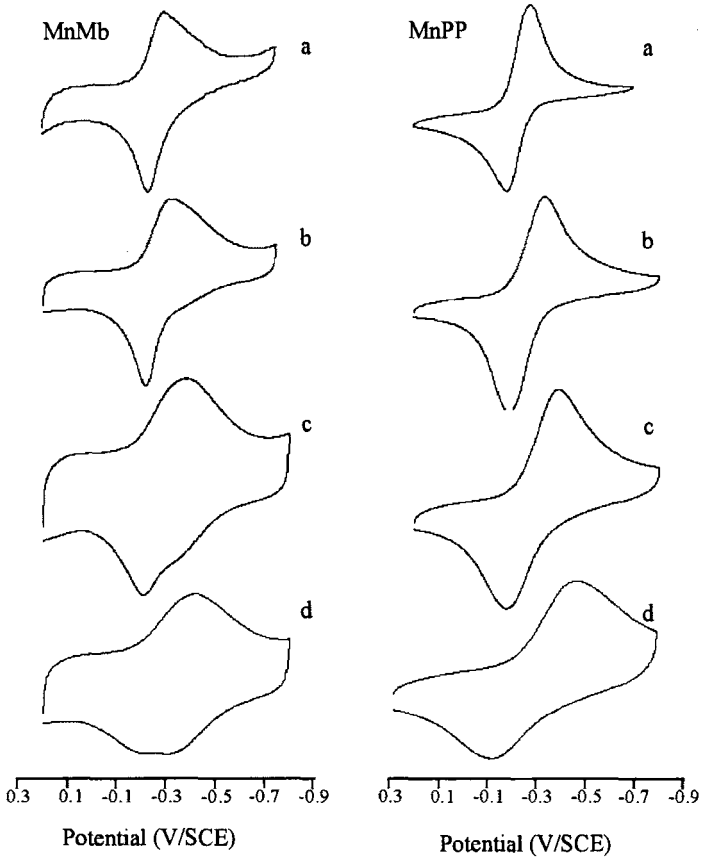


FIGURE 6 Voltammograms of MnMb and MnPP in pH 7.0 buffer, 0.5 M NaBr at scan rates of (a) 5 mV/s; (b) 50 mV/s; (c) 500 mV/s; (d) 5 V/s

## CATALYSIS BY MB/DDAB

Mb/ddab electrodes catalytically reduce aqueous solutions of oxygen, nitrite and sulfite, as illustrated by the CVs in Fig. 7. The large rise in current in the presence of substrate indicates an increase in the number of electrons passed per Fe site, i.e., the catalytic turnover. We hope to utilize this system to understand the course of these reactions in a con-

tained, protein environment. The remainder of this Comment will focus on our efforts to characterize the catalytic reduction of nitrite by Mb/ddab. But first a brief, and by no means complete, description of the enzymatic systems is in order.

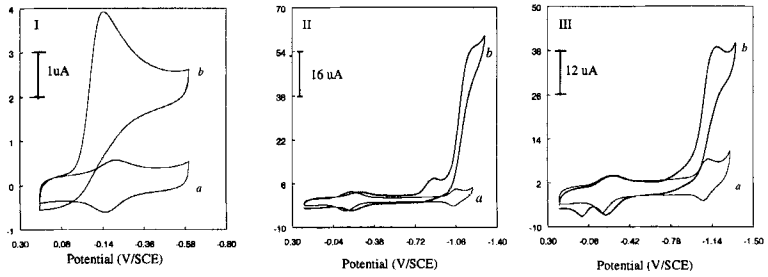


FIGURE 7 Voltammograms of myoglobin with (I) $O_2$; (II) 5 mM $NaNO_2$; (III) 5 mM $Na_2SO_3$. Scan a-myoglobin only; Scan b-in the presence of substrate. Conditions: at 100 mV/sec, pH 2.0 buffer, 0.05 M NaBr



Heme-based nitrite reductases (NiR) are integral to the biochemical cycling of nitrogen, transforming $NO_2^-$ to a variety of reduced products.[29–31] The assimilatory enzymes produce $NH_4^+$ for incorporation into biomass,[3] while the dissimilatory enzymes function as terminal electron acceptors or to detoxify the inorganic ions (Scheme 3).[30] The dissimilatory NiR are often involved in multienzyme denitrification processes which include other heme-based enzymes such as nitric oxide reductases, NoR, and nitrous oxide reductases, NoS. Such processes are of importance in the bacterial decomposition of soil fertilizers (a major source of atmospheric $N_2O$) and in the industrial removal of $NO_x$ pollutants from wastewater.[31]

$$NO_2^- + 7\,H^+ \xrightarrow{6\,e^-} NH_3 + 2\,H_2O \qquad \textbf{assimilatory}$$

$$NO_2^- \xrightarrow{[\,e^-\,]} NH_3 + NO + N_2O + N_2 \qquad \textbf{dissimilatory}$$

SCHEME 3

The assimilatory NiR activity involves multiple proton-coupled reductions, typically at Fe-siroheme active sites.[32] All the reductases have associated redox sites such as $Fe_4S_4$ clusters or other Fe-heme sites which aid in the multi-electron reductions of the substrate. The overall stoichiometry, involving six electron reductions, is shown in Scheme 4 as sequential two-electron steps as proposed by Cowan with the second [Fe] representing a coupled $Fe_4S_4$ cluster.[32] The formation of dissimilatory, substrate-coupled products (e.g., $N_2O$) has been attributed to the reactivity of partially reduced intermediates in this sequential pathway.

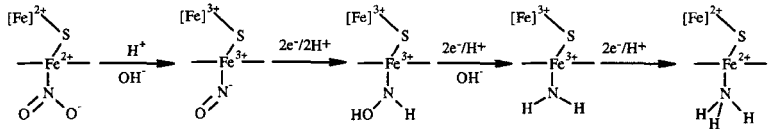


SCHEME 4

Fe-heme and other transition metal complexes have been used as models for this catalysis.[21,33] Meyer, in particular, has investigated water-soluble Fe-porphyrins and other metal complexes as catalysts for the electroreduction of nitrite. To our knowledge only one report of nitrite reductase activity by other heme proteins has been made.[34]

For Mb/ddab catalysis of nitrite reduction, there are three waves seen in the CV in Fig. 7IIb which give information on the course of the reaction.[35] The reversible $Fe^{III/II}$couple shifts to lower potentials, demonstrating nitrite binding at the Fe site. The next two waves, labeled I and II in Fig. 8, are both catalytic, corresponding to ca. 20 and 220 electrons per Fe site at peak current in Fig. 8a. Also, there is a distinctly different effect of pH on the two catalytic waves, illustrated in Fig. 8. The small potential shift and large current decrease with pH for wave II suggests a multi-electron, multi-proton process. Both catalytic waves also demonstrate saturation kinetics, i.e., the current increases with substrate concentration up to a maximum value. This enzyme-like behavior yields a Michealis constant, $K_m$, of 2.3 mM, close to the $K_d$ of 3 mM for nitrite binding to Mb in solution.[23,35]

We have identified $NH_3$ and $NH_2OH$ as aqueous products of bulk electrolysis at potentials corresponding to catalytic wave II. Mass spectral analysis of the headgas over electrolyzed solutions of $^{15}NO_2^-$ shows

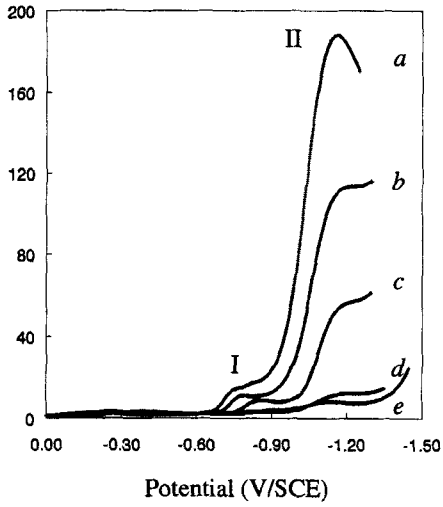


FIGURE 8 Linear sweep voltammograms at 100 mV/sec of Mb/ddab in 3 mM $NaNO_2$ and 0.5 M buffers at (a) pH 5.09; (b) pH 6.00; (c) pH 6.76; (d) pH 7.82; (e) pH 8.96



strong signals for $^{15}N_2O$, and that smaller amounts of $^{15}NO$ and $^{15}N_2$ are also produced.[36]

To test which oxidation state is associated with the N-N coupled gas formation in Mb/ddab catalysis, we monitored the headgas above $^{15}NO_2^-$ solution while sparging with He under bulk electrolysis conditions. Potentials corresponding to ferrous Mb yield no discernible gas production over long time periods (> 30 min). Upon stepping the potential to that associated with catalytic wave I, a strong ion abundance due to $N_2O$ was observed. No dramatic acceleration of $N_2O$ production was observed by stepping the potential to a value corresponding to catalytic wave II, but the production of $N_2$ and NO was seen.

The reactivity of Mb/ddab is quite similar to that found by Meyer *et al.* in the catalytic reduction of nitrite by water-soluble Fe-porphyrins (e.g., $Fe^{II}$-tetra(4-sulfonatophenyl)-porphyrin)$^{4-}$ in acidic solutions [Eq. (1)].[21a,b] An important difference is the formation of $Fe^{III}$-NO from dehydration of nitrite by the ferrous catalyst [Eq. (2)]. CVs of Meyer's catalyst in nitrite solutions showed a greatly diminished anodic current at the $Fe^{III/II}$ couple, a result of the depletion of $Fe^{II}$(TPPS) by Eq. (2),

and also a growth of waves corresponding to the nitrosyl. They estimated the equilibrium constant $K$ at $> 2 \times 10^{14}$ $M^{-1}$ for Eq. (2).

$$NO_2^- \xrightarrow[[e^-]]{[FeTPPS]^{4-}} NH_3 + NH_2OH + N_2O + N_2(< 1\%) \quad (1)$$

$$[Fe^{II}(H_2O)TPPS]^{4-} + HONO + H^+ \rightarrow [Fe^{III}(NO)TPPS]^{3-} + H_2O \quad (2)$$

We see no evidence for such a nitrite/nitrosyl conversion from the ferrous Mb/ddab state. Though shifted cathodically, the $Fe^{III/II}$ couple remains quite reversible in the presence of nitrite (Fig. 7IIb), even at the slowest scan rates. It is well known that MbNO can be formed from metMb and nitrite in the presence of excess reductant,[37] but in our system nitrite dehydration only occurs at potentials which form the stable $Fe^{II}$-NO as the kinetic product, i.e., by a direct reduction of the ferrous rather than the ferric-nitrite complex. This suggests the active-site pocket or the film environment kinetically inhibits $Fe^{III}$-NO formation. Isoelectronic with $Fe^{II}$-CO, $Fe^{III}$- NO would prefer linear Fe-N-O coordination to maximize $\pi$-backbonding. The destabilization of linear $Fe^{II}$-CO binding in Mb leads to a $10^3$ decrease in $K_d$ when compared to Fe(TPP)CO;[38] a large destablization is also known for metMb as compared with $Fe^{III}(TPPS)^{3-}$.[39]

As an $Fe^{II}$-NO Mb complex is a likely intermediate in reductions of nitrite, we ran CVs of Mb/ddab in solutions saturated with NO gas (Fig. 9). These show significant differences from CVs in the presence of nitrite. The $Fe^{III/II}$ wave is absent after the initial scan due to the ready formation of $Fe^{II}$-NO. We do not see oxidation to $Fe^{III}$-NO under these conditions (to 400 mV), which again suggest this species is disfavored in Mb/ddab. A strong catalytic wave appears ca. –0.7 V at pH 7, well positive to that of nitrite's first catalytic wave. And in contrast to nitrite reduction, this first NO reduction is catalytic from pH 5 to 10. The second reduction wave resembles that for nitrite, approximately the same potential and a high current flow, suggestive of a multiple-electron reduction step past the $Fe^{II}$-$NO^-$, or nitroxyl state. Mass spectral analysis of the headgas during bulk electrolysis by Mb/ddab electrodes of NO saturated solutions showed formation of $N_2O$ at potentials associated with the first catalytic wave.

$$2[Fe^{II}(NO^-)(TPPS)]^{5-} \rightarrow [(TPPS)Fe^{II}(N_2O_2^{2-})Fe^{II}(TPPS)]^{10-} \rightarrow N_2O + 2[Fe^{III}(H_2O)(TPPS)]^{4-} \quad (3)$$

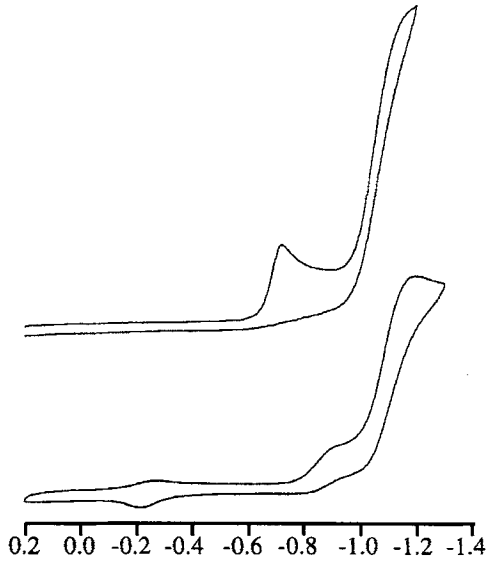


FIGURE 9 Voltammograms of Mb/ddab in the presence of a) ca. 1.5 mM NO; b) 5 mM nitrite. Conditions: 100 mV/sec, 0.5 M pH 7.0 phosphate buffer, 0.5 M NaBr

Meyer *et al.* attributed the $N_2O$ seen during nitrite reduction by Fe-porphyrins to bimolecular dimerization between reduced nitroxyl ($Fe^{II}$-$NO^-$) [Eq. (3)].[21a–c] Such coupling in our system is precluded by the protein-isolated active sites. Two paths remain for the $N_2O$ production catalyzed by Mb/ddab: coupling at a single Fe site or by reduced $NO_x$ species in solution (Scheme 5). Similar considerations have long been argued in the N-N coupling reactions relevant to the denitrification processes,[29,30] and more recently in the mechanisms of the heme-based nitric oxide reductase, NoR enzymes.[40,41] A possible mode of coupling at a single Fe-site is seen in Scheme 5. Such coupling of NO with an X-$NO^-$ anion is precedented in the formation of NONOates, as in Angeli's salts.[42] Alternatively, free $NO^-$ released into solution is known to rapidly dimerize, forming hyponitrous acid which then decomposes to $N_2O$ and water.[43] Efforts to distinguish between the two pathways by analysis of concentration and pH dependence data are underway.[44]

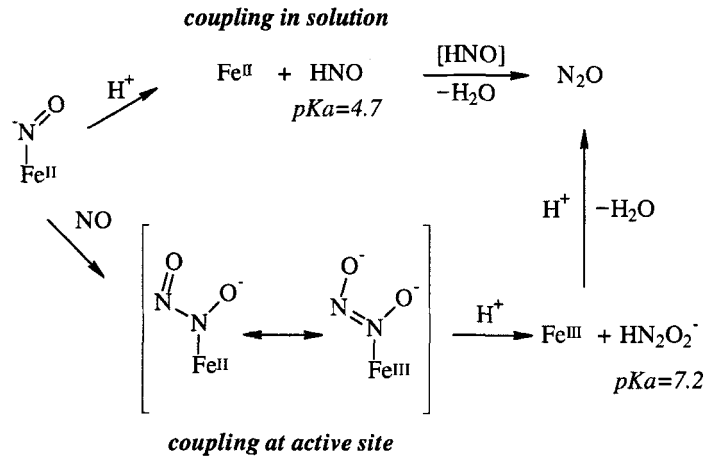


SCHEME 5



These results yield several insights into the nitrite reduction catalysis by Mb/ddab, and are combined into the overall reaction shown in Scheme 6. The first catalytic reduction wave from $Fe^{II}$-$NO_2^-$ includes both reductive dehydration forming $Fe^{II}$-NO and subsequent reduction to the $Fe^{II}$-$NO^-$ nitroxyl state. The lack of reductive catalysis at high pH must be due primarily to inhibition of the initial dehydration step. As suggested in previous model studies, the nitroxyl state partitions between a further reduction to yield $NH_3$ and the coupling path leading to $N_2O$.[21] The ready formation of $N_2O$ from nitrite without evidence of free NO argues for solution-based coupling of $NO^-$. Thus far attempts to intercept free $NO^-$ in solution and thus retard $N_2O$ production during Mb/ddab nitrite reductions have been unsuccessful.[44,45] Further reduction from the nitroxyl state leads to formation of $NH_3$. The formation of $NH_2OH$ and $N_2$ implies reactivities associated with other partially reduced intermediates; tentative precursors, such as the $Fe^V$-nitrido, which may lead to these products are shown. We have no evidence of intermediate states other than that assigned to the nitroxyl on the time-scales of our experiments.

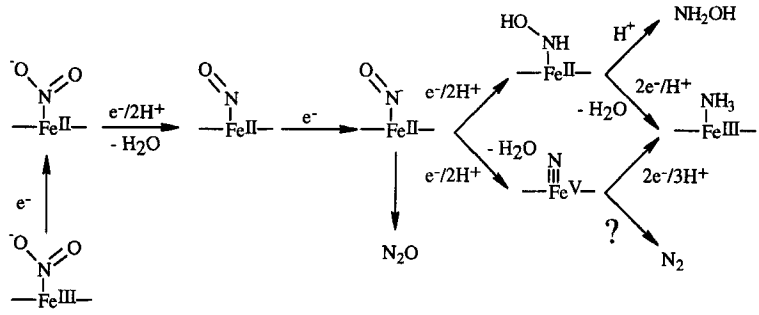


SCHEME 6

## CONCLUSIONS

The electrochemistry of Mb in surfactant films is unique in several ways. Especially significant is the ability to access a highly reduced $Fe^{I}$ state, and still undergo facile binding and exchange of aqueous ligands. Excellent current response allows detection of chemical transformations accompanying electron transfer down to the millisecond timescale. The protein pocket of Mb influences both the reversible electron transfers to the metal site as well as the course of catalytic transformations that occur there. The use of Mb/ddab as a hemeprotein NiR model yields products characteristic of both enzymatic pathways. Importantly, the reductive dimerization of NO by Mb/ddab, likely through a nitroxyl intermediate, can occur at potentials within physiological regime, ca. −500 mV on the NHE scale. Thus Mb/ddab holds promise as a system with which biomimetic catalysis can be studied electrochemically within a modifiable protein environment.

*Abbreviations:* Mb – myoglobin; ddab – dimethyldidodecylammonium bromide; PG – pyrolytic graphite; CV – cyclic voltammetry; OSWV – Osteryoung square wave voltammetry; SCE – standard calomel electrode; His – histidine TPP – tetraphenylporphyrin; PP – protoporphyrin IX; TPPS – tetrakis(4-sulfonatophenyl)-porphyrin)$^{4-}$; NiR – nitrite reductase.

**Acknowledgments**

Financial support for this research was provided by a grant from the National Science Foundation (CHE-9629938) and departmental startup funds from the University of California, Irvine.

**References**

1. (a) S. I. Chan and P. M. Li, Biochem. **29**, 1 (1990). (b) B. G. Malstrom and R. Aasa, FEBS **325**, 49 (1993). (c) G. T. Babcock and M. Wikstrom, Nature (London) **356**, 301 (1992).
2. (a) J. H. Dawson, Science **240**, 433 (1988). (b) T. D. Porter and M. H. Coon, J. Biol.Chem. **266**, 13469 (1991). (c) M. Akhtar and J. N. Wright, Nat. Prod. Rep. **8**, 527 (1991).
3. (a) M. G. Guerrero, J. M. Vega and M. Losada, Ann. Rev. Plant Physiol. **32**, 169 (1981). (b) T. Brittain, R. Blackmore, C. Greenwood and A. J. Thomson, Euro. J. Biochem. **209**, 793 (1992)
4. (a) T. A. Hansen and I. Anonie Van Leeu, J. Gen. Mol. Microbiol. **66**, 165 (1994). (b) B. R. Crane, L. M. Siegel and E. D. Getzoff, Science, **270**, 59 (1995). (c) I. Moura and A. R. Lino, Meth. Enzym. **243**, 296 (1994).
5. One exception is cytochrome P450BM3, which accepts two electrons from NADH. J. T. Hazzard, S. Govindaraj, T. L. Poulos and G. Tollin, J. Biol.Chem. **272**, 7922 (1997).
6. For many wonderful examples, see: (a) C. Amatore, in *Organometallic Radical Processes*, W. C. Trogler, Ed., 1990 (Elsevier Science Publishing Comp. New York), Chp. 1. (b) D. Astruc, in *Electron Transfer and Radical Processes in Transition-Metal Chemistry,* 1995 (VCH Publishers, Inc., New York), Chp. 6 and 7.
7. F. A. Armstrong, J. Biol. Inorg. Chem. **2**,139 (1997).
8. (a) L. H. Guo and H. A. O. Hill, Adv. Inorg. Chem. **36**, 341 (1991). (b) F. M. Hawkridge and I. Taniguchi, Comm. Inorg. Chem. **17**, 163 (1995). (c) H. A. O. Hill, Coord. Chem. Rev. **151**, 115 (1996).
9. F. A. Armstrong, J. N. Butt and A. Sucheta, Meth. Enzym. **227**, 479 (1993).
10. M. Collinson and E. F. Bowden, Langmuir **8**, 1247 (1992).
11. (a) J. F. Rusling and A. E. F. Nassar, J. Am. Chem. Soc. **115**, 11891 (1993). (b) A. E. F. Nassar, W. S. Willis and J. F. Rusling, Anal. Chem. **67**, 2386 (1995). (c) A. E. F. Nassar, J. M. Bobbitt, J. D. Stuart and J. F. Rusling, J. Am. Chem. Soc. **117**, 10986 (1995).
12. (a) J. F. Rusling, A. E. F. Nassar and T. F. Kumosinski, ACS Symposium Series **576**, 250 (1994). (b) A. E. F. Nassar, Z. Zhang, V. Chynwat, H. A. Frank, J. F. Rusling and K. Suga, J. Phys. Chem. **99**, 11013 (1995). (c) A. E. F. Nassar, Y. Narikiyo, T. Sagara, N. Nakashima and J. F. Rusling, J. Chem. Soc. Faraday Trans. **91**, 1775 (1995). (d) A. E. F. Nassar, Z. Zhang, N. Hu, J. F. Rusling and T. F. Kumonsinski, J. Phys. Chem. B. **101**, 2224 (1997).
13. (a) C. L. Miaw, N. F. Hu, J. M. Bobbit, Z. K. Ma and M. F. Ahmadi, Langmuir **9**, 315 (1993). (b) J. F. Rusling, C. L. Miaw and E. C. Couture, Inorg. Chem. **29**, 2025 (1990).
14. Z. Zhang, A.-E. F. Nassar, Z. Lu, J. B. Schenkman and J. F. Rusling J. Chem. Soc. Faraday Trans. **93**, 1769, (1997).

15. (a) B. R. Dyke, P. Saltman and F. A. Armstrong, J. Am. Chem. Soc. **118**, 3490 (1996). (b) D. D. Schlereth and W. Mantele, Biochem. **31**, 7494 (1992). (c) J. N. Ye and R. P. Baldwin, Anal. Chem. **60**, 2263 (1988).
16. A. J. Bard, in *Integrated Chemical Systems: A Chemical Approach to Nanotechnology*, 1994 (Wiley, New York), Chp 5.
17. (a) D. Lexa, M. Momenteau and J. Mispelter, Biochim. Biophys. Acta **338**, 151 (1974). (b) I. A. Cohen, D. Ostfeld and B. Lichtenstein, J. Am. Chem. Soc. **94**, 4522 (1971). (c) S. G. Srvatsa, D. T. Sawyer, N. J. Boldt and D. F. Bocian, Inorg. Chem. **24**, 2125 (1985).
18. K. M. Kadish, in *Iron Porphyrins, Part II*, A. B. P. Lever and H. B. Gray, Eds., 1983 (Addison-Wesley, Reading, MA), Chp. **4**.
19. T. Inubushi and T. Yonetani, Meth. Enzym. **76**, 88 (1981).
20. J. A. Cowan and H. B. Gray, Inorg. Chem. **28**, 2074 (1989).
21. (a) W. R. Murphy Jr., K. Takeuchi, M. H. Barley and T. J. Meyer, J. Am. Chem. Soc. **104**, 5817 (1982). (b) M. H. Barley, K. Takeuchi and T. J. Meyer, J. Am. Chem. Soc. **108**, 5876 (1986). (c) M. H. Barley, M. R. Rhodes and T. J. Meyer, Inorg. Chem. **26**, 1746 (1987). (d) J. N. Younathan, K. S. Wood and T. J. Meyer, Inorg. Chem. **31**, 3280 (1992).
22. E. Antonini and M. Brunori, in *Hemoglobin and Myoglobin in Their Reactions with Ligands*, 1971 (North-Holland Publishing Company, Amsterdam), Chp 9.
23. M. Sono and J. H. Dawson, J. Biol. Chem. **257**, 5496 (1982).
24. B. C. King, F. M. Hawkridge and B. M. Hoffman, J. Am. Chem. Soc. **114**, 10603 (1992).
25. (a) Y. Shiro, T. Iwata, R. Makino, M. Fujii,Y. Isogai and T. Iizuka, J. Biol. Chem. **268**, 19983 (1993). (b) A. M. Bracete, M. Sono and J. H. Dawson, Biochim. Biophys. Acta **1080**, 264 (1991). (c) N. Kamiya, Y. Shiro, T. Iwata, T. Iizuka and H. Iwasaki, J. Am. Chem. Soc. **113**, 1826 (1991).
26. M. J. Natan. D. Kuila, W. W. Baxter, B. C. King, F. M. Hawkridge and B. M. Hoffman, J. Am. Chem. Soc. **112**, 4081 (1990).
27. X. H. Mu and F. A. Schultz. Inorg. Chem. **29**, 2879 (1990).
28. N. Parthasarathi and T. G. Spiro, Inorg. Chem. **26**, 3792 (1987).
29. (a) B. A. Averill, Chem. Rev. **96**, 2951 (1996). (b) R. W. Ye, B. A. Averill and J. M. Tiedje, Appl. Envir. Microbiol. **60**, 1053 (1994).
30. (a) S. Ferguson, J. Anton. Leeuw. **66**, 89 (1994). (b) Y. Henry and P. Bessieres, Biochimie **66**, 259 (1984).
31. W. J. Payne in *Denitrification*, 1981 (John Wiley & Sons, New York).
32. (a) S. M. Lui, W. Liang, A. Soriano and J. A. Cowan, J. Am. Chem. Soc. **116**, 4531 (1994). (b) S. M. Lui, W. Liang, A. Soriano and J. A. Cowan, J. Am. Chem. Soc. **115**, 10483 (1993).
33. (a) J. E. Toth and F. C. Anson, J. Am. Chem. Soc. **111**, 2444 (1989). (b) M. R. Rhodes, M. H. Barley and T. J. Meyer, Inorg. Chem. **30**, 629 (1991). (c) S. Sunohara, K. Nishimura, K. Yahikozawa, M. Ueno, M. Eny and Y. Takasu, J. Electroanal. Chem. **354**, 161 (1993). (d) B. Keita, A. Belhouari, L. Nadjo and R. Constant, J. Electroanal. Chem. **381**, 243 (1995). (e) Y. Liu and M. D. Ryan, J. Electroanal. Chem. **368**, 209 (1994).
34. K. Miki, T. Ikeda and H. Kinoshita, Electroanal. **6**, 703 (1994).
35. R. Lin. M. Bayachou. J. Greaves and P. J. Farmer. submitted for publication.
36. Both $[^{15}NO]^+$and $[^{15}N_2]^+$ are produced by $^{15}N_2O$ ionization in the MS, but varying abundance ratios measured during electrolysis deviated substantially from those obtained by ionization of an authentic $^{15}N_2O$ sample. Separation of sampled headgas aliquots by a GC column prior to ionization confirm independent $^{15}NO$ and $^{15}N_2$ production during electrolysis.

37. E. V. Arnold and D. S. Bohle, Meth. Enzym. **269**, 41 (1996).
38. G. B. Jameson and J. A. Ibers, in *Bioinorganic Chemistry*, I. Bertini, H. B. Gray. S. J. Lippard and J. S. Valentine, Eds., 1994 (University Science Books, Mill Valley), Chp 4, pp. 238–240.
39. M. Hoshino, K. Ozawa, H. Seki and P. C. Ford, J. Am. Chem. Soc. **115**, 9568 (1993).
40. Y. Shiro, M. Fujii, T. Iizuka, S. Adachi, K. Tsukamoto, K. Nakahara and H. Shoun. J. Biol. Chem. **270**, 1617 (1995).
41. M. Dermastia, T. Turk and T. C. Hollocher. J. Biol. Chem. **266**, 10899 (1991).
42. L. K. Deefer, D. Christodoulou, T. M. Dunams, J. A. Hrabie, C. M. Maragos, J. E. Saavedra and D. A. Wink, in *Nitrosamines and Related N-Nitroso Compounds: Chemistry and Biochemistry,* R. N. Loepky and C. J. Michejda, Eds., 1994, ACS Symposium Series 553 (American Chemical Society, Washington, DC), Chp 11.
43. M. N. Hughes and G. Stedman, J. Chem. Soc. 1239 (1963).
44. M. Bayachou, R. Lin and P. J. Farmer, manuscript in preparation.
45. J. Goretski and T. C. Hollocher, J. Biol. Chem. **263**, 2316 (1988).